Nature **363**, 509 (1993)] have shown significantly lower NO and higher ClO concentrations than had been predicted by models that did not include heterogeneous processes.
2. The addition of a single reaction, the heterogeneous hydrolysis of N_2O_5 (reaction 1), to the photochemical data set used in stratospheric models results in a shift away from an NO_x-dominated lower stratosphere. In these models, NO_x catalysis still dominates O_3 loss above 24 km. [See, for example, M. B. McElroy, R. J. Salawitch, K. Minschwaner, *Planet. Space Sci.* **40**, 373 (1992); J. M. Rodriguez *et al.*, *Geophys. Res. Lett.* **21**, 209 (1994), and references therein].
3. J. G. Anderson and O. B. Toon, *Geophys. Res. Lett.* **20**, 2499 (1993).
4. J. F. Gleason *et al.*, *Science* **260**, 523 (1993).
5. R. S. Stolarski and H. L. Wesoky, Eds., *NASA Ref. Publ. No. 1313* (1993).
6. D. R. Bates and M. Nicolet, *J. Geophys. Res.* **55**, 301 (1950).
7. The mixing ratio is the fraction of total molecules in a given volume. At the pressure and temperature typical of the ER-2 cruise altitude, there are approximately 2×10^{18} molecules cm^{-3}. Thus, 1 pptv is equivalent to a concentration of 2×10^6 molecules cm^{-3}.
8. R. M. Stimpfle *et al.*, *Geophys. Res. Lett.* **17**, 1905 (1990).
9. P. O. Wennberg *et al.*, *Rev. Sci. Instrum.* **65**, 1858 (1994).
10. P. O. Wennberg *et al.*, unpublished results.
11. C. R. Webster, R. D. May, C. A. Trimble, R. G. Chave, J. Kendall, *Appl. Opt.* **33**, 454 (1994).
12. D. W. Fahey *et al.*, *J. Geophys. Res.* **94**, 11299 (1989); R. Gao *et al.*, *ibid.*, in press.
13. C. R. Webster *et al.*, *ibid.* **95**, 13851 (1990).
14. R. C. Cohen *et al.*, in preparation. The concentration of $HONO_2$, which is required in this model, is inferred from the measurements of reactive nitrogen, NO_y, by assuming:

$$[HONO_2] \approx [NO_y] - [NO] - [NO_2] - [ClONO_2]$$

$[ClONO_2]$ is calculated by assuming photochemical steady state (Eq. 12). N_2O_5 is neglected because of its small mixing ratio.
15. A photochemical steady state exists when the lifetime [concentration ÷ production (or loss) rate], is short; production is balanced by removal on short time scales. The radical species have short lifetimes, typically less than 1 hour, whereas some molecular species, such as $HONO_2$ or O_3 have lifetimes of months to years in the lower stratosphere.
16. R. J. Salawitch *et al.*, *Geophys. Res. Lett.*, in press.
17. L. Jaeglé *et al.*, *ibid.*, in press.
18. We speculate that an acid-catalyzed aerosol reaction of pernitric acid (PNA, $HOONO_2$) could be a source of HONO. Although reactions of PNA on sulfuric acid aerosols have never been studied, Z. Li, R. R. Friedl, and S. P. Sander [in preparation] have shown that PNA is adsorbed on ice with high efficiency ($\gamma = 0.15 \pm 0.10$ at 190 K). Salawitch *et al.*, show that an assumed γ of 0.2 ± 0.1 results in an excellent match to the high zenith angle OH observations (*16*). This process increases the diurnally averaged HO_x concentration in two ways: (i) it reduces an important sink (OH reacts quickly with PNA); and (ii) it redistributes HO_x to high zenith angles, where its lifetime is longer. Additionally, this process would be a nonnegligible sink for O_3 in the lower stratosphere.
19. W. B. DeMore *et al.*, *Jet Propul. Lab. Publ. 92-20* (1992).
20. BrO is measured by the Harvard resonance fluorescence experiment [W. H. Brune, J. G. Anderson, K. R. Chan, *J. Geophys. Res.* **94**, 16639 (1989).] Because of the small BrO concentrations, long integration periods (typically 20 min or more) are required to achieve signal-to-noise ratios of greater than 2. We have used the [BrO] measurements from SPADE and the earlier AASE II campaign to develop a climatology. Measured BrO concentrations for all sunlit flights are consistent with the relation: $[BrO] = 0.45 (\pm 0.1) \times [Br_y]$. Br_y is the total available inorganic bromine ($BrO + HOBr + BrONO_2 + HBr + Br$) and is inferred from the measured $[N_2O]$ with the method described by E. L. Woodbridge *et al.* for inorganic chlorine (*27*).
21. R. Toumi, R. L. Jones, J. A. Pyle, *Nature* **365**, 37 (1993). For these calculations, we have used a quantum yield for NO_3 formation of 0.5, in line with the most recent laboratory work [see, for example, T. K. Minton, C. M. Nelson, T. A. Moore, M. Okumura, *Science* **258**, 1342 (1992)].
22. Additional O_3 loss occurs through the reaction of O with O_3. In addition to O_2 photolysis, production of O_3 occurs through the oxidation of CH_4 (and other hydrocarbons) in the presence of NO. These processes, although largely negligible, are included in the production and removal rates shown in Fig. 4.
23. R. J. Salawitch *et al.*, *Geophys. Res. Lett.*, in press.
24. This net removal rate can be compared with that inferred from Microwave Limb Sounder (MLS) ozone measurements. Under conditions of extreme chlorine activation, net removal rates in the arctic polar vortex during February 1993 (2 months before the measurements reported here) were estimated to be 20% per month [G. L. Manney *et al.*, *Nature* **370**, 429 (1994)].
25. R. C. Cohen *et al.*, *Geophys. Res. Lett*, in press.
26. R. M. Stimpfle *et al.*, *ibid.*, in press.
27. E. L. Woodbridge *et al.*, *J. Geophys. Res.*, in press. Correlations between the long-lived tracer N_2O and organic chlorine compounds measured by gas chromatography (GC) are used to estimate the total organic chlorine and, by inference, the available inorganic chlorine. The GC measurements were made aboard the ER-2 during the SPADE and AASE II deployments by J. W. Elkins of the NOAA aeronomy laboratory. Additionally, whole air samples taken by S. M. Schauffler and L. E. Heidt of NCAR during AASE II included measurements of organic bromine compounds.
28. This inference of the $ClONO_2$ concentration leads to difficulties in balancing the inorganic chlorine budget. In particular, measured HCl concentrations are usually lower than predicted by this estimate of the $ClONO_2$ concentration [see C. R. Webster *et al.*, *Science* **261**, 1130 (1993)].
29. A. R. Douglass *et al.*, *NASA Ref. Publ. No. 1251* (1991).
30. In situ measurements of the distribution of long-lived tracers such as those made during SPADE can be used to place constraints on dynamical transport rates, a key issue in determining the distribution and lifetime of O_3 [K. A. Boering *et al.*, *Geophys. Res. Lett.*, in press; S. C. Wofsy *et al.*, *ibid.*, in press; E. Hintsa *et al.*, *ibid.*, in press].
31. We thank the pilots (W. Collette, J. Barrilleaux, D. Krumrey, J. Nystrum, and R. Williams) and the ground crews of the ER-2, without whom this work would not have been possible. ER-2 flight planning by P. A. Newman and co-workers from NASA-Goddard was instrumental to the success of SPADE. The TOMS UV reflectivity is produced by R. D. McPeters and co-workers of the NASA-Goddard ozone processing team; L. Pfister at NASA-Ames was responsible for interpolating this data onto the ER-2 flight track. New instrumentation for OH and HO_2 was developed in part by N. L. Hazen, L. B. Lapson, N. T. Allen, J. F. Oliver, N. W. Lanham, J. N. Demusz, E. E. Thompson, T. L. Martin, E. M. Weinstock, and A. E. Dessler at Harvard University. Interface with the ER-2 was supported by H. Kent, G. Prince, and R. York, at Lockheed; their efforts are gratefully acknowledged. Program support at NASA-Ames by J. C. Arveson, J. L. Barrilleaux, E. Condon, S. Wegner, and S. Hipskind is acknowledged. Finally, this work was supported by the NASA High Speed Research Program, under the direction of H. L. Wesoky, R. S. Stolarski, and M. J. Prather. Additional support for the HO_x instrument development came from the NASA Upper Atmosphere Research Program, under the direction of M. J. Kurylo.

6 June 1994; accepted 1 September 1994

TLC1: Template RNA Component of *Saccharomyces cerevisiae* Telomerase

Miriam S. Singer and Daniel E. Gottschling

Telomeres, the natural ends of linear eukaryotic chromosomes, are essential for chromosome stability. Because of the nature of DNA replication, telomeres require a specialized mechanism to ensure their complete duplication. Telomeres are also capable of silencing the transcription of genes that are located near them. In order to identify genes in the budding yeast *Saccharomyces cerevisiae* that are important for telomere function, a screen was conducted for genes that, when expressed in high amounts, would suppress telomeric silencing. This screen lead to the identification of the gene *TLC1 (telomerase component 1). TLC1* encodes the template RNA of telomerase, a ribonucleoprotein required for telomere replication in a variety of organisms. The discovery of *TLC1* confirms the existence of telomerase in *S. cerevisiae* and may facilitate both the analysis of this enzyme and an understanding of telomere structure and function.

Telomeres are specialized nucleoprotein complexes that constitute the ends of eukaryotic chromosomes and protect chromosomes from degradation and end-to-end fusion (*1*, *2*). When telomeres are absent, the instability of nontelomeric chromosomal ends leads to chromosome loss (*3*). In addition, telomeres are required for the complete replication of chromosomes (*1*, *2*, *4*).

DNA polymerases synthesize DNA in a 5′ to 3′ direction and require a primer to initiate synthesis. These restrictions pose a problem for the complete replication of linear chromosomes (*5*). In the absence of a specialized mechanism to maintain termi-

The authors are in the Department of Molecular Genetics and Cell Biology, The University of Chicago, Chicago, IL 60637, USA.

nal sequences, multiple replication cycles would cause chromosomes to shorten progressively from their ends. In many eukaryotes, telomeres are composed of simple tandem repeats, with the 3′-terminal strand composed of G-rich sequences (*1*, *2*). Insight into the mechanism by which telomeric DNA is maintained has come from the identification of telomerase activity in several species of ciliates, as well as in extracts of *Xenopus*, mouse, and human cells (*6*). Telomerase is a ribonucleoprotein enzyme that elongates the G-rich strand of chromosomal termini by adding telomeric repeats (*4*). This elongation occurs by reverse transcription of a part of the telomerase RNA component, which contains a sequence complementary to the telomere repeat. After the telomerase-catalyzed extension of the G-rich strand, the complementary DNA (cDNA) strand of the telomere is presumably replicated by more conventional means.

Telomerase is now the focus of increasing interest, because of reports linking it to cellular senescence and oncogenesis (*7*). Germline cells, whose chromosomal ends must be maintained through repeated rounds of DNA replication, do not decrease their telomere length with time, presumably as a result of the activity of telomerase (*8*). In contrast, somatic cells appear to lack telomerase, and their telomeres shorten with multiple cell divisions (*8–10*). The repression of telomerase activity in somatic cells may have a critical role in the control of the number of times that they divide. Indeed, the length of telomeres in primary fibroblasts correlates well with the number of divisions these cells can undergo before they senesce (*8*). The loss of telomeric DNA may signal to the cell the end of its replicative potential, as part of an overall mechanism by which multicellular organisms limit the proliferation of their cells. Conversely, late stage tumors probably require the reactivation of telomerase in order to avoid total loss of their telomeres and massive destabilization of their chromosomes. Immortalized cell lines produced from virally transformed cultures have active telomerase and stable telomere lengths (*10*). Recently, telomerase activity has also been detected in human ovarian carcinoma cells (*11*).

The evolutionary conservation of telomere structure suggests that the study of telomerase in genetically tractable organisms, such as the budding yeast *Saccharomyces cerevisiae*, may yield general insight. Although no telomerase activity has yet been identified in yeast extracts, results from a recent genetic study suggested the existence of an *S. cerevisiae* telomerase (*12*). In that work, double-strand breaks were introduced into yeast chromosomes in vivo. The healed chromosomes, to which the cell had added new telomeric tracts, were then analyzed. A specific 13–base pair (bp) motif (GTGTGTGGGTGTG) or an 11-bp subset of this sequence were frequently found at the junction between the break site and the new telomeric tracts, which suggests that this sequence is added de novo. It was predicted that the RNA template component of the putative yeast telomerase would contain the sequence complementary to this motif.

In spite of evidence suggesting an overall mechanism for telomeric replication in *S. cerevisiae*, little is known about the molecular machinery of this process. Until now, the only candidate for a component of the telomere replication apparatus has been the protein encoded by the *EST1* gene (*13*). Its role in telomere replication is suggested by the finding that *est1* cells display progressive telomere shortening, which is accompanied by a gradual loss of chromosome stability and cell viability. The direct function of Est1p is not yet known.

A screen for suppressors of telomeric silencing. Genes located near *S. cerevisiae* telomeres are subject to transcriptional silencing by a repressive chromatin structure that initiates at the telomeres (*14–16*). We proposed that the telomeric structure responsible for silencing might be a multimeric complex that would be sensitive to the stoichiometric imbalance of its components. Therefore, in order to identify genes involved in telomere structure or function, we carried out a screen for gene products that, when expressed at high amounts, would suppress telomeric silencing. A yeast strain was constructed with genetic markers located at two telomeric loci. The *ADE2* gene, which is required for adenine biosynthesis, was placed adjacent to the telomere at the right arm of chromosome V (V-R), and *URA3*, a gene required for uracil biosynthesis, was located adjacent to the telomere at the left arm of chromosome VII

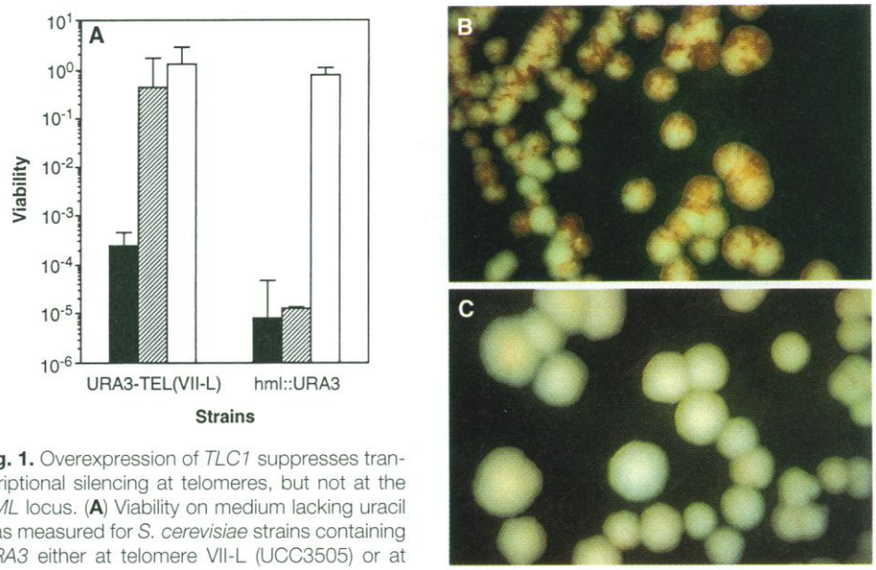

Fig. 1. Overexpression of *TLC1* suppresses transcriptional silencing at telomeres, but not at the *HML* locus. (**A**) Viability on medium lacking uracil was measured for *S. cerevisiae* strains containing *URA3* either at telomere VII-L (UCC3505) or at *HML* (UCC3515), and overexpressing either vector alone (pTRP, black bar), a representative *TLC1* cDNA clone (pTRP6, hatched bar), or a *SIR4* cDNA clone (pTRP10, white bar) (*41*). *ADE2* expression, as assayed by colony color, was examined in cells containing *ADE2* placed near telomere V-R (UCC3505), and containing either (**B**) the vector (pTRP), or (**C**) another representative *TLC1* cDNA clone (pTRP61). The medium contained 3 percent galactose and lacked tryptophan.

Fig. 2. Overexpression of *TLC1* causes a decrease in telomeric tract length. Yeast strain UCC3505 carrying either vector (pTRP, lanes 1 and 2) or a *TLC1* cDNA clone (pTRP6, lanes 3 and 4) were pregrown for approximately 60 generations on medium containing 3 percent galactose without tryptophan. Genomic DNA was prepared from two independent transformants of each strain, digested with Apa I and Xho I, separated by electrophoresis on a 1 percent agarose gel, and blotted onto a nylon membrane. The membrane was probed with a 1.1-kb Hind III–Sma I *URA3* fragment. The *URA3* gene in this strain is located adjacent to telomere VII-L. The higher molecular weight (nontelomeric) *URA3* fragments represent sequences of the telomeric *URA3* that are centromere-proximal to the *URA3* Apa I site, and sequences from the *ura3-52* allele at the normal chromosomal locus of *URA3* (42). The telomeric fragment is indicated by the arrow.

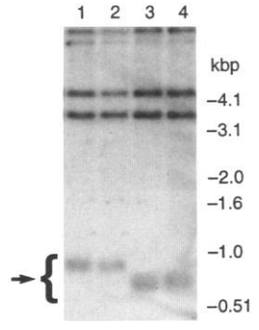

(VII-L) (*17*). Normally, colonies expressing *ADE2* are white, whereas those not expressing it (*ade2*) are red (*18*). As a result of the semistable nature of telomeric silencing of most genes, switching between silenced and transcriptionally active states may occur every few generations and thus give rise to different phenotypic populations. In the case of strains with *ADE2* located near a telomere, these different populations are seen as red and white sectors within a single colony (*14*). A *URA3* gene located at telomere VII-L also normally switches between transcriptional states (*14*). However, we caused the telomeric *URA3* to be completely silenced by deleting its trans-activator, *PPR1* (*19*). The cells were therefore unable to grow in the absence of uracil.

To identify genes or gene fragments whose overexpression could disrupt silencing, the strain was transformed with a high-expression *S. cerevisiae* cDNA library (*20*). Because the nature of its synthesis, a cDNA library typically contains both full-length and truncated versions of RNA transcripts. Thus high-level expression from a cDNA library has two means of causing a stoichiometric imbalance: by expression of a normal gene product or a defective one (*21*). In the library used in our study, the expression of cDNA inserts was controlled by the *GAL1* promoter, which is strongly induced by the presence of galactose in the medium (*22*). Of the 330,000 yeast transformants we obtained, 48 displayed a galactose-dependent decrease in telomeric silencing. That is, when grown on media containing galactose, the cells were able to grow in the absence of uracil (Ura^+) and gave rise to predominantly white colonies (Ade^+). On the basis of restriction mapping, DNA blotting (Southern) analysis, and DNA sequencing, we determined that these 48 clones represented ten independent genes (*23*).

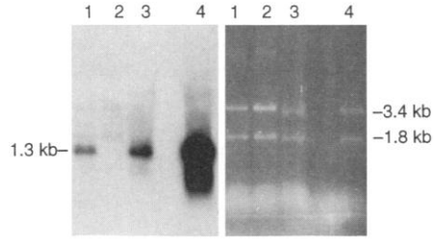

Fig. 3. *TLC1* encodes a 1.3-kb RNA. *TLC1* transcript levels were analyzed in yeast strains containing a wild-type *TLC1* gene (lane 1), or a *tlc1::LEU2* disruption allele (lane 2), and in wild-type cells carrying either vector (pTRP, lane 3) or a *TLC1* cDNA clone (pTRP61, lane 4). Total RNA was isolated from mid-log phase cells grown in rich medium (for strains lacking plasmids) or in synthetic medium without tryptophan but with 3 percent galactose (for the plasmid-containing strains). RNA (20 μg) from each strain was electrophoretically separated on a 0.9 percent agarose formaldehyde gel, transferred to a nylon membrane, probed with a 1.25-kb *TLC1* antisense probe (made from the pTRP61 insert), and exposed to film (left). Phosphorimaging analysis determined that there is approximately 12 times more *TLC1* RNA in the overexpressing strain (lane 4) than in the vector-containing wild-type strain grown under the same conditions (lane 3). The right panel displays the ethidium bromide–stained gel prior to blotting, with the sizes of the rRNA species (25S and 18S) indicated on the right. The wild-type and *tlc1* strains shown in lanes 1 and 2 were derived from sporulation of UCC3508 (*31*). The yeast strain transformed with the pTRP and pTRP61 plasmids, shown in lanes 3 and 4, is UCC3505.

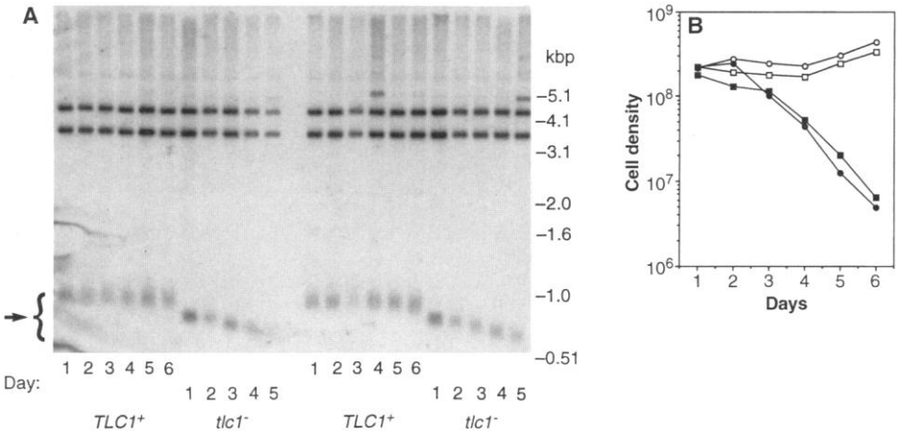

Fig. 4. Disruption of *TLC1* causes progressive telomere shortening and a gradual decrease in growth rate and viability. (**A**) A *TLC1/tlc1::LEU2* diploid (UCC3508) was sporulated and the resulting tetrads were dissected and germinated on rich medium. Colonies representing the four spore products from a tetrad were inoculated into 5.5 ml of rich medium and grown at 30°C. Every 24 hours, 5 ml of the culture were used for the preparation of genomic DNA, and 5 μl were used to inoculate 5.5 ml of fresh medium. The genomic DNA was digested with Apa I, electrophoresed on a 1 percent agarose gel, transferred to a nylon membrane and hybridized to a 1.1-kb *URA3* probe. The *URA3* gene is located adjacent to telomere VII-L in these strains (*43*). The telomeric fragment is indicated with an arrow. (**B**) In an experiment similar to that described above, UCC3508 spore products were grown continuously in rich medium. Every 24 hours, the cell density was determined and each culture was diluted to 3×10^5 cells per milliliter in 5.5 ml of fresh medium for further growth. The cell density at each time point is plotted for the two *TLC1* (white circle and square) and *tlc1* (black circle and square) spore products of a tetrad.

Isolation of *TLC1*, a telomere-specific suppressor of silencing. The genes known to be required for telomeric silencing are also involved in transcriptional silencing at two internal chromosomal sites, the *HML* and *HMR* loci, which harbor the unexpressed copies of the mating type genes in *S. cerevisiae* (*24*). To determine whether the newly isolated suppressors of telomeric silencing also affect silencing at *HML*, the expression plasmids were introduced into a strain in which the *URA3* gene was inserted into the *HML* locus (*25*). Overexpression of one of the genes identified, *TLC1*, had no effect on silencing at *HML*, but strongly suppressed telomeric silencing of *URA3* and *ADE2* (Fig. 1). The *SIR4* gene, whose overexpression disrupts silencing both at telomeres and at *HML* (*26*), was also isolated in our screen and derepressed both of these loci in our assay (Fig. 1).

Further evidence for the specific association of *TLC1* with telomere structure came from an examination of telomere length in strains overexpressing a *TLC1* cDNA clone. In the absence of the *TLC1* overexpression plasmid, the telomeric sequences at VII-L averaged 330 bp in length. When *TLC1* was overexpressed, the average telomere length at VII-L decreased between 90 and 220 bp (Fig. 2). The alteration of telomere length on overexpression of *TLC1*, together with the loss of telomeric silencing, suggested that this gene is specifically involved in telomere structure.

Of the 48 cDNA clones isolated in our screen as suppressors of telomeric silencing, nine represented *TLC1*. Physical mapping localized *TLC1* to a single site on chromosome II, immediately adjacent to *CSG2* (*27*, *28*). We sequenced one of the *TLC1* cDNA clones in its entirety (pTRP61, 1248 bp), as well as the ends of the other eight *TLC1* clones. These sequence data overlapped to yield a contiguous sequence of 1301 bp, although no single clone included the entire sequence (*29*). After this work was completed, the sequence of chromosome II was entered into the EMBL database (*30*). These data match the sequence that we had obtained from the cDNAs. RNA blot (Northern) analysis confirmed that a wild-type strain contained a relatively abundant RNA that hybridized to a *TLC1* probe and was approximately 1.3 kb in length (Fig. 3).

Encoding of the *S. cerevisiae* telomerase RNA by *TLC1*. The *TLC1* sequence

has two notable features. The gene does not seem to encode a protein because it does not contain a large open reading frame (ORF). The longest ORF that begins with an ATG codon is only 43 amino acids in length. This finding suggested that the functional *TLC1* gene product might be the RNA itself. Moreover, *TLC1* contains the sequence CACCACACCCACACAC, which includes the motif predicted to template *S. cerevisiae* telomeres (*12*). These results suggested that *TLC1* encodes the putative yeast telomerase RNA.

If the *TLC1* gene product is indeed the telomerase RNA, then disruption of *TLC1* would be predicted to cause incomplete replication of telomeres, which would result in progressive telomere shortening with each cell division. A *TLC1* disruption was created in which a large part of *TLC1*, including the predicted telomere-templating region, was removed and replaced with a marker gene (*31*). This disruption was introduced into a wild-type diploid strain to create a *TLC1/tlc1* heterozygote, which was then sporulated, giving rise to two mutant and two wild-type haploid strains. Northern analysis confirmed that in the *TLC1*-disrupted spore products, there was no detectable *TLC1* RNA (Fig. 3). The spore colonies were inoculated into rich medium and grown for several days by diluting the cultures into fresh medium every 24 hours. In all cases examined (eight tetrads), *TLC1* strains maintained a normal telomere length after 6 days of growth. In contrast, the *tlc1* strains displayed shortened telomeres. In the cases in which DNA samples were collected daily (three tetrads), the *tlc1* telomeres shortened progressively, at an approximate rate of 3 bp per generation (Fig. 4A).

In conjunction with the shortening telomere phenotype, older *tlc1* cultures displayed a gradual increase in generation time. Through the first 40 generations after sporulation of a *TLC1/tlc1* strain, all four spore products were able to regrow approximately one thousand–fold in rich medium within 24 hours, an indication that the generation time was less than 2.4 hours (Fig. 4B). This growth rate was maintained in *TLC1* strains for up to 80 generations. In the *tlc1* strains, however, by 65 generations after germination the growth rate had slowed to about 3.3 hours per generation. After 75 generations, the doubling time of the *tlc1* cultures was 5.7 hours. This decrease in growth rate was accompanied by a 50 percent drop in viability in the *tlc1* strains after 75 generations (*23*). This general pattern was clear in all 14 tetrads examined although there was some variation in the period at which the decrease in growth rate occurred. However, as was reported for *est1* strains (*32*), the dying *tlc1* cultures were overtaken within approximately 100 generations by faster-growing cells, which presumably contained suppressor mutations (*23*).

To determine whether the *TLC1* gene product is the *S. cerevisiae* telomerase template RNA, it was necessary to confirm that *TLC1* sequences encode telomeric tract repeats. Earlier experiments with *Tetrahymena thermophila* showed that when a mutated telomerase RNA is introduced into a cell, the altered sequence may be used as a template and incorporated into the telomeres of the cell (*33*). A candidate motif for the telomere template within *TLC1* was the sequence CACCACACCCACACAC (Fig. 5A). We constructed a *TLC1* allele, designated *TLC1-1(Hae III)*, in which two base pairs of this motif were changed to create a recognition site for the restriction enzyme Hae III (Fig. 5B). This mutant allele was used to replace one of the normal *TLC1* genes in a diploid strain (*34*).

In addition to functioning at the very ends of normal telomeres, telomerase is also believed to participate in the healing of broken chromosomes and in the extension of unusually short telomeric tracts (*12*). In this latter capacity, the activity of a mutant telomerase would be most easily detected. Therefore, fragment-mediated transformation was used to remove the sequence distal

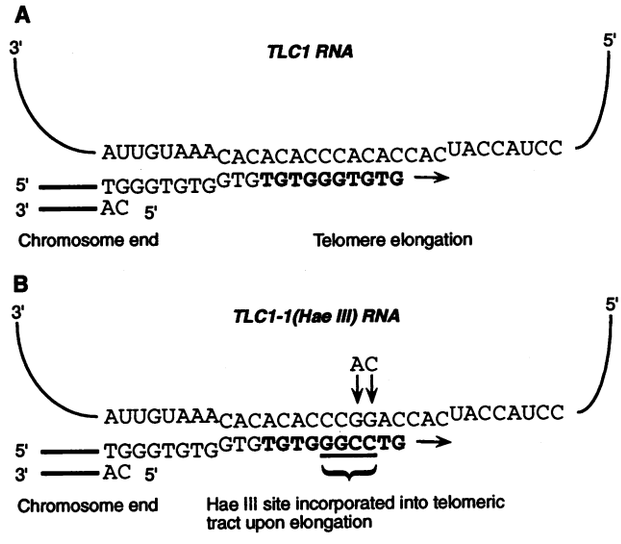

Fig. 5. The *TLC1* gene is proposed to encode an RNA that functions as a templating component of telomerase, an enzyme that elongates the G-rich strand of *S. cerevisiae* telomeres (**A**). By this model, the *TLC1* RNA anneals to the single-stranded G-rich overhanging strand at the end of the chromosome and templates its elongation by means of a reverse transcription reaction. The bold-type DNA bases represent newly synthesized sequence. (**B**) In accordance with this hypothesis, it is predicted that mutating the putative template motif of *TLC1*, creating the *TLC1-1(Hae III)* allele, should result in the incorporation of the altered sequence into telomeric DNA.

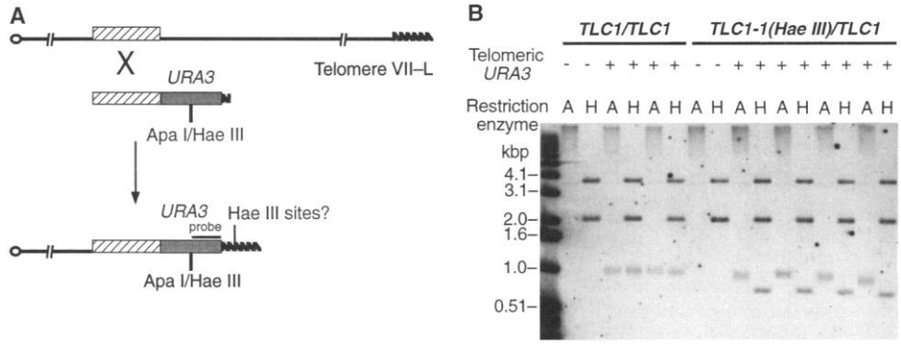

Fig. 6. Altering the putative telomere-templating region of *TLC1* results in the incorporation of the mutant sequence into telomeric tracts. (**A**) Fragment-mediated transformation of *TLC1/TLC1* and *TLC1-1(Hae III)/TLC1* diploid strains was used to replace the terminal sequences of the left arm of one of the chromosome VII homologs with a *URA3* gene and a short telomeric tract sequence. The most telomere-proximal Apa I and Hae III sites in the fragment used in the transformation overlap and are located 0.75 kb from the telomeric end of the fragment. (**B**) Restriction digests of genomic DNA from transformed strains were used to determine whether Hae III sites were introduced into the new telomere VII-L upon its elongation in vivo. Genomic DNA from *TLC1/TLC1* and *TLC1-1(Hae III)/TLC1* yeast strains, either transformed with URA3TEL (telomeric *URA3*$^+$) or not (telomeric *URA3*$^-$), was digested with Apa I (A) or Hae III (H). The DNA fragments were separated by electrophoresis on a 1.25 percent agarose gel, transferred to a nylon membrane, and probed with a labeled 0.6-kb *URA3* probe (Apa I–Hind III fragment), as depicted in (A). Each telomeric *URA3*$^+$ strain represents an independently isolated transformant.

to the *ADH4* locus on the left arm of chromosome VII, and replace it with a *URA3* gene and a short tract of telomeric sequence to act as a seed for in vivo telomere elongation (Fig. 6A). This transformation was done in both homozygous wild-type (*TLC1/TLC1*) and heterozygous *TLC1-1(Hae III)/TLC1* strains (*35*). Southern analysis was performed on genomic DNA from the transformed strains to determine the structure of the new telomeres at VII-L (Fig. 6B). Digestion with Apa I, whose most distal site in the new VII-L arm occurs within the *URA3* gene, demonstrated that, in both the wild-type (*TLC1/TLC1*) and heterozygous *TLC1-1(Hae III)/TLC1* transformants, the new chromosomal end was extended in vivo to several hundred base pairs. The new telomeres in the *TLC1-1(Hae III)/TLC1* strains were slightly shorter and more heterogeneous in length than those added in the *TLC1/TLC1* strains. In all 12 *TLC1/TLC1* independent transformants tested, digestion with Hae III, which cuts at the same site in *URA3* as Apa I, indicated that no Hae III sites were introduced during telomere elongation in vivo. In contrast, in all eight *TLC1-1(Hae III)/TLC1* independent strains examined, Hae III sites were incorporated into the newly formed telomere. We conclude that the mutated sequence in the *TLC1-1(Hae III)* gene served as a template for the addition of telomeric repeats, which indicates that the *TLC1* gene indeed encodes the *S. cerevisiae* telomerase RNA.

Comparison of *TLC1* with other telomerase RNAs. In our study we have demonstrated the existence of an *S. cerevisiae* telomerase and have identified the gene that encodes its RNA component. Our findings support the theory that the telomerase mechanism of replicating the ends of chromosomes is widespread among eukaryotes. However, the *TLC1* RNA is much larger (1.3 kb) than the known ciliate telomerase RNAs, which are 160 to 200 nucleotides (nt) in length (*4*). This discrepancy in gene size is reminiscent of the 1175-nt *S. cerevisiae* U2 small nuclear RNA (snRNA), which is almost 1 kb larger than the mammalian U2 snRNA (*36*). The conserved secondary structure that is shared among the ciliate telomerase RNAs is not apparent in the sequences surrounding the *TLC1* template region (*37*), although the large size of the transcript may allow homologous structures, that are not obvious at this time, to form. Also, *TLC1* lacks a short primary sequence adjacent to the template region that is conserved among the ciliate telomerase RNAs (*38*).

Whereas telomeric DNA in most organisms consists of sequences repeated in a regular fashion [for example, mammalian (T_2AG_3), *Tetrahymena* (T_2G_4)], the telomeric sequence of *S. cerevisiae* is irregular [$(TG)_{1-3}TG_{2-3}$] (*1*). However, this irregularity can be fully explained by the telomere-templating sequence in *TLC1*. Telomerase RNAs are thought to synthesize the G-rich strand of telomeres by multiple rounds of hybridization to a short sequence at the end of a telomeric tract, elongation of the DNA by a limited reverse transcription of the RNA, and disengagement (*4*). In vitro, the *Tetrahymena* telomerase RNA appears to use as few as three nucleotides for the hybridization step (*39*). The telomere template region of *TLC1* (CACCACACCCACACAC) suggests that the telomerase RNA may be able to align with a telomere terminus at a number of different points within the RNA, especially if CAC is all that is required for hybridization. It is also possible that the telomerase could abort a round of reverse-transcription at several different positions along the RNA. If a terminal DNA sequence such as GTG is left, then alignment with the CAC RNA motif in the next round of elongation can readily occur. Either alone or in combination, these different alignment and termination possibilities can account for the heterogeneity observed in the *S. cerevisiae* telomeric tracts.

A link between telomeric silencing and telomerase. Overexpression of the *TLC1* cDNA clones identified in our study both disrupts telomeric silencing and causes a shortening of telomeres. One model to explain these results is that overexpression of the cDNAs causes limiting telomerase components to be titrated into incomplete and nonfunctional complexes, thereby reducing the total telomerase activity in the cell and resulting in shorter telomeres. The length of the telomere may relate to its ability to bind silencing proteins; shorter telomeres simply have fewer binding sites, and thus may silence telomeric genes less efficiently (*40*). Alternatively, the telomerase RNA itself, or one of the factors it binds, may be an integral component of the complex that is required for silencing at telomeres. Overexpression of *TLC1* may perturb the stoichiometry of this complex, and thus interfere with its assembly. Of the nine *TLC1* cDNAs isolated in our screen, none appear to be full length (*29*). Thus it is formally possible that only an incomplete (nonfunctional) *TLC1* RNA can produce the effects detected.

The telomere shortening and growth defects that we observed when the telomerase RNA was disrupted are very similar to those described for *est1* strains; this observation lends further support to the prediction that *EST1* is a constituent of telomerase (*13*). Moreover, the genetic link discovered here between telomeric silencing and telomerase suggests future approaches for identifying other telomerase components, which so far have been elusive.

REFERENCES AND NOTES

1. V. A. Zakian, *Annu. Rev. Genet.* **23**, 579 (1989).
2. E. H. Blackburn, *Nature* **350**, 569 (1991); C. M. Price, *Curr. Opin. Cell Biol.* **4**, 379 (1992); E. R. Henderson and D. D. Larson, *Curr. Opin. Gen. Dev.* **1**, 538 (1991); J. H. Wright, D. E. Gottschling, V. A. Zakian, *Genes Dev.* **6**, 197 (1992); E. H. Blackburn, *Cell* **77**, 621 (1994).
3. L. L. Sandell and V. A. Zakian, *Cell* **75**, 729 (1993).
4. E. H. Blackburn, in *The RNA World*, R. F. Gesteland and J. F. Atkins, Eds. (Cold Spring Harbor Laboratory Press, Cold Spring Harbor, NY, 1993), pp. 557–576.
5. J. D. Watson, *Nature New Biol.* **239**, 197 (1972); A. M. Olovnikov, *J. Theor. Biol.* **41**, 181 (1973).
6. C. W. Greider and E. H. Blackburn, *Cell* **43**, 405 (1985); *ibid.* **51**, 887 (1987); *Nature* **337**, 331 (1989); A. M. Zahler and D. M. Prescott, *Nucleic Acids Res.* **16**, 6953 (1988); G. B. Morin, *Cell* **59**, 521 (1989); K. R. Prowse, A. A. Avilion, C. W. Greider, *Proc. Natl. Acad. Sci. U.S.A.* **90**, 1493 (1993); D. Shippen-Lentz and E. H. Blackburn, *Mol. Cell. Biol.* **9**, 2761 (1989); L. L. Mantell and C. W. Greider, *EMBO J.* **13**, 3211 (1994).
7. T. de Lange, *Proc. Natl. Acad. Sci. U.S.A.* **91**, 2882 (1994); C. W. Greider, *Curr. Opin. Gen. Dev.* **4**, 203 (1994); C. B. Harley, H. Vaziri, C. M. Counter, R. C. Allsopp, *Exp. Gerontol.* **27**, 375 (1992).
8. R. C. Allsopp *et al., Proc. Natl. Acad. Sci. U.S.A.* **89**, 10114 (1992).
9. C. B. Harley, A. B. Futcher, C. W. Greider, *Nature* **345**, 458 (1990); N. D. Hastie *et al., Nature* **346**, 866 (1990); J. Lindsey, N. I. McGill, L. A. Lindsey, D. K. Green, H. J. Cooke, *Mut. Res.* **256**, 45 (1991); H. Vaziri *et al., Am. J. Hum. Genet.* **52**, 661 (1993).
10. C. M. Counter *et al., EMBO J.* **11**, 1921 (1992); J. W. Shay, W. E. Wright, D. Brasiskyte, B. A. Van Der Haegen, *Oncogene* **8**, 1407 (1993); A. J. Klingelhutz, S. A. Barber, P. P. Smith, K. Dyer, J. K. McDougall, *Mol. Cell. Biol* **14**, 961 (1994); C. M. Counter, F. M. Botelho, P. Wang, C. B. Harley, S. Bacchetti, *J. Virol.* **68**, 3410 (1994).
11. C. M. Counter, H. W. Hirte, S. Bacchetti, C. B. Harley, *Proc. Natl. Acad. Sci. U.S.A.* **91**, 2900 (1994).
12. K. M. Kramer and J. E. Haber, *Genes Dev.* **7**, 2345 (1993).
13. V. Lundblad and J. W. Szostak, *Cell* **57**, 633 (1989).
14. D. E. Gottschling, O. M. Aparicio, B. L. Billington, V. A. Zakian, *Cell* **63**, 751 (1990).
15. D. E. Gottschling, *Proc. Natl. Acad. Sci. U.S.A.* **89**, 4062 (1992).
16. H. Renauld *et al., Genes Dev.* **7**, 1133 (1993).
17. The strain used for transformation with the library was UCC3505 (*MATa ura3-52 lys2-801 ade2-101 trp1-Δ63, his3-Δ200 leu2-Δ1 ppr1::HIS3 adh4::URA3-TEL DIA5-1); DIA5-1* refers to the directed integration of *ADE2* adjacent to telomere V-R. The UCC3505 strain was constructed by successively transforming YPH499 [R. S. Sikorski and P. Hieter, *Genetics* **122**, 19 (1989)] with pVII-L URA3-TEL (*14*), pΔPPR1-HIS3 (*16*), and pHR10-6. Plasmid pHR10-6 (provided by H. Renauld) was constructed by inserting a 2.8-kb Hind III fragment from plasmid pV-R URA3-TEL (*14*) (which contained sequences from the subtelomeric region of chromosome arm V-R) into the Hind III site of pYTCA-2 (*14*), such that the Eco RI site of the insert was furthest from the Bam HI site of the vector, thus creating pHR9-9. Into the Bam HI site of pHR9-9 we inserted the 3.4-kb Eco RI–Bam HI fragment containing the *ADE2* gene from pL909 (*14*), thus creating pHR10-6. The *ADE2* gene is thus oriented with its promoter proximal to the V-R sequences. Plasmid pHR10-6 was cleaved with Eco RI for use in fragment-mediated transformation of yeast.
18. H. Roman, *Cold Spring Harbor Symp. Quant. Biol.* **21**, 175 (1956).
19. O. M. Aparicio and D. E. Gottschling, *Genes Dev.* **8**, 1133 (1994).
20. The pTRP plasmid expression library used in our study was created with *cre-lox* site-directed recom-

bination from the λTRP library (provided by S. J. Elledge, Baylor College of Medicine, Houston). The pTRP vector contains a 2μ origin of replication and the *TRP1* selectable marker. The cDNA inserts were cloned into a Xho I site of the pTRP vector, placing them under the control of the *GAL1* promoter. The creation of similar libraries was described [S. J. Elledge, J. T. Mulligan, S. W. Ramer, M. Spottswood, R. W. Davis, *Proc. Natl. Acad. Sci. U.S.A.* **88**, 1731 (1991)].

21. I. Herskowitz, *Nature* **329**, 219 (1987).
22. M. Johnston and R. W. Davis, *Mol. Cell. Biol.* **4**, 1440 (1984).
23. M. S. Singer and D. E. Gottschling, unpublished data.
24. O. M. Aparicio, B. L. Billington, D. E. Gottschling, *Cell* **66**, 1279 (1991).
25. The strain used for assaying silencing at the *HML* locus was UCC3515 *(MATα lys2-801 ade2-101 trp1-Δ63 his3-Δ200 leu2-Δ1 ura3-52 hml::URA3).* The *hml::URA3* construct was the same as that described for strain GJY5 [D. J. Mahoney and J. R. Broach, *Mol. Cell. Biol.* **9**, 4621 (1989)].
26. M. Marshall, D. Mahoney, A. Rose, J. B. Hicks, J. R. Broach, *Mol. Cell. Biol.* **7**, 4441 (1987); H. Renauld and D. E. Gottschling, unpublished results.
27. *TLC1* was mapped by hybridizing the labeled cDNA clone (1.25 kb Xho I insert from pTRP6) to a filter grid containing λ phage clones representing more than 96 percent of the yeast genome. The filter set was obtained from the American Type Culture Collection [M. V. Olson *et al., Proc. Natl. Acad. Sci. U.S.A.* **83**, 7826 (1986); A. J. Link and M. V. Olson, *Genetics* **127**, 681 (1991)].
28. T. Beeler, K. Gable, C. Zhao, T. Dunn, *J. Biol. Chem.* **269**, 7279 (1994).
29. The combined sequence of the *TLC1* cDNA clones has been submitted to GenBank and assigned the accession number U14595. The span of each of the cDNA clones with respect to the entire 1301-bp fragment is as follows: pTRP6 (1 to 1248), pTRP61 (54 to 1301), pTRP14 and pTRP47 (54 to 1263), pTRP33 and pTRP39 (54 to 1269), pTRP55 (54 to 1264 or 1265), pTRP59 (39 to 1250), and pTRP60 (270 to 1264 or 1265). For reference, the CACCACACCCACACAC template sequence spans the region 468 to 483. Four of the *TLC1* cDNA sequences (in clones pTRP55, pTRP60, pTRP33, and pTRP39) are followed by short stretches (5 to 20 nt) of adenine nt. It is not yet clear whether these adenine nt reflect authentic in vivo polyadenylation of the *TLC1* transcripts, or are by-products of cDNA synthesis.
30. The chromosome II-R sequences have the EMBL accession number X76078.
31. The *TLC1* cDNA clone in plasmid pTRP61 was excised from pTRP vector sequences as a 1.25-kb Xho I fragment, and inserted into the Xho I site of pBluescript II KS(−) (Stratagene; La Jolla, CA), creating pBlue61. The disruption of *TLC1* was created by replacing the 693-bp Nco I–Nsi I fragment of pBlue61 with a blunt-ended Bam HI 1.6-kb *LEU2* clone from plasmid YDp-L [G. Berben, J. Dumont, V. Gilliquet, P. Bolle, F. Hilger, *Yeast* **7**, 475 (1991)], creating pBlue 61::LEU2. This construct was digested with Xho I and transformed into the dipolid strain UCC3507, and Leu$^+$ transformants were selected for, resulting in the production of UCC3508 (UCC3507 *TLC1/tlc1::LEU2).* Southern blot analysis confirmed that UCC3508 was heterozygous for the disruption at the *TLC1* locus. Of 19 tetrads sporulated from UCC3508, all yielded 2:2 segregation of the *tlc1::LEU2* allele. The genotype of UCC3507 is: *MATa/MATα ura3-52/ura3-52 lys2-801/lys2-801 ade2-101/ade2-101 his3-Δ200/his3-Δ200 trp1-Δ1/TRP1 leu2-Δ1/leu2-Δ1 adh4::URA3-TEL/adh4::URA3-TEL DIA5-1/ DIA5-1 ppr1::HIS3/ppr1::LYS2.* The hap- loid strains crossed to create UCC3507 were derived from YPH250 and YPH102 [R. S. Sikorski and P. Hieter, *Genetics* **122**, 19 (1989)]. The introduction of changes into the genotypes of these haploids utilized the plasmids described above, except allele *ppr1::LYS2*, which was introduced with the use of plasmid pΔPPR1::LYS2 (*16*).
32. V. Lundblad and E. H. Blackburn, *Cell* **73**, 347 (1993).
33. G.-L. Yu, J. D. Bradley, L. D. Attardi, E. H. Blackburn, *Nature* **344**, 126 (1990).
34. Plasmid pVZ61b was constructed by inserting the 1.25-kb Xho I fragment containing the *TLC1* cDNA clone from pTRP61 into the Sal I site of plasmid pVZ1 [S. Henikoff and M. K. Eghtedarzadeh, *Genetics* **117**, 711 (1987)]. The *TLC1-1(Hae III)* mutant allele was generated with the use of two oligonucleotides, Hpa I primer (5′-TCCAGAGTTAACGATAAGATAGAC-3′) and Hae III(6-7) primer (5′-TAATTACCATGGGAAGCCTACCATCACCAGGCCCACA CACAAATG-3′) to amplify by PCR (polymerase chain reaction) a 232-bp fragment from plasmid pVZ61b. The PCR product was then cleaved with Nco I and Hpa I, to create a 213-bp fragment that was used to replace the 213-bp Nco I–Hpa I fragment of pBlue61, to create pBlue61–Hae III(6-7). The 213-bp fragment was sequenced from the pBlue61 plasmid to verify that the PCR amplification did not introduce additional mutations into the sequence. The *TLC1-1(Hae III)* allele, contained in a 1.25-kb Xho I fragment, was cleaved from pBlue61-Hae III(6-7) and inserted into the Xho I site of pRS306 [R. S. Sikorski and P. Hieter, *Genetics* **122**, 19 (1989)], to create the integrating plasmid pRS306-TLC1-1(Hae III). This construct was digested with Afl II and used to transform YPH501 (R. S. Sikorski and P. Hieter, *ibid.*), with selection for Ura$^+$ transformants, thus creating the heterozygous strain UCC3520. UCC3522 [YPH501 *TLC1-1(Hae III) TLC1*] was isolated as a 5-fluoro-orotic acid–resistant derivative of UCC3520 in which the pRS306-TLC1 plasmid had recombined out of the *TLC1* locus, which left the *TLC1-1(Hae III)* allele in the chromosome [S. Scherer and R. W. Davis, *Proc. Natl. Acad. Sci. U.S.A.* **76**, 4951 (1979)], as confirmed by Southern blot analysis.
35. The *ADH4-URA3*-TG_{1-3} fragment used to replace the left arm of chromosome VII was generated by Not I–Sal I digestion of plasmid AD3ARUGT-IV. This plasmid was constructed by the following set ot steps: the 1.1-kb Hind III–Sma I DNA fragment containing *URA3* [M. Rose, P. Grisafi, D. Botstein, *Gene* **29**, 113 (1984)] was inserted into the Hinc II site of pYTCA-2 by blunt-end ligation, with the promoter of *URA3* proximal to the TG_{1-3} sequences of the vector, creating plasmid p3ARUCA. The 1.2-kb Hind III fragment of pYA4-2, containing *ADH4* [(*13*); V. M. Williamson and C. E. Paquin, *Mol. Gen. Genet.* **209**, 374 (1987)], was then inserted into the Hind III site of p3ARUCA, with the Sal I site of the insert distal to the *URA3* gene in the vector, creating plasmid pAD3ARUCA. Finally, the Sal I–EcoR I fragment containing the composite insert (ADH4-URA3-TG_{1-3}) from pAD3ARUCA was cloned into pVZ1, creating AD3ARUGT-IV. The yeast strains that were transformed with the *ADH4-URA3*-TG_{1-3} fragment were YPH501 (*TLC1/TLC1)* and UCC3522 [*TLC1-1(HaeIII)/TLC1*]. These experiments were repeated with the transforming *ADH4-URA3*-TG_{1-3} DNA liberated from the pAD3ARUGT-IV plasmid as a Sal I–EcoR I fragment, and results similar to those reported in Fig. 6B were obtained.
36. M. Ares, *Cell* **47**, 49 (1986).
37. D. P. Romero and E. H. Blackburn, *Cell* **67**, 343 (1991); E. ten Dam, A. van Belkum, K. Pleij, *Nucleic Acids Res.* **19**, 6951 (1991).
38. J. Lingner, L. L. Hendrick, T. R. Cech, *Genes Dev.* **8**, 1984 (1994).
39. C. Autexier and C. W. Grieder, *ibid.*, p. 563.
40. G. Kyrion, K. Liu, C. Liu, A. J. Lustig, *ibid.* **7**, 1146 (1993).
41. The median value for viability in the absence of uracil is marked by the height of each column, and the upper extreme is indicated by the error bar. The strains were first grown for 4 days on solid synthetic medium without tryptophan (to maintain selection for the plasmid) that contained 3 percent galactose (to induce the *GAL1* promoter controlling expression of the cDNA inserts). Colonies were then diluted in water, and serial dilutions were plated on 3 percent galactose medium without tryptophan and uracil. Cells were also plated on medium containing uracil, to determine overall cell viability. Five independent transformants of each strain were tested.
42. The Southern blot was also probed with an 81-bp–labeled $(TG)_{1-3}TG_{2-3}$ (telomeric sequence) riboprobe, to determine the telomere length of chromosomes with Y′ elements [R. W. Walmsley, C. S. M. Chan, B.-K. Tye, T. D. Petes, *Nature* **310**, 157 (1984)]. These telomere-associated sequences are at the ends of multiple yeast chromosomes and generally have Xho I sites at their telomere-proximal ends [E. J. Louis and J. E. Haber, *Genetics* **124**, 533 (1990)]. Y′-containing chromosomes showed a decrease of telomere length upon overexpression of the *TLC1* cDNA clone similar to that seen above for telomere VII-L.
43. In a similar experiment, genomic DNA from *TLC1* and *tlc1* cultures was digested with Xho I, as well as Apa I, in order to examine Y′-containing telomeres by the method described (*42*). The size of this population of telomeres decreased at the same rate as the *URA3*-labeled telomere VII-L.
44. We thank S. Elledge for providing the λTRP library; and C. Atcheson, B. Berg, S. Diede, A. Kahana, L. Meisinger, M. Parthun, M. A. Singer and J. Stevenson for helpful comments on the manuscript. Supported by a Medical Scientist National Research Service Award and a National Defense Science and Engineering Graduate Fellowship (M.S.S.); a Pew Charitable Trust Biomedical Scholars Fellowship and National Institutes of Health grant GM43893 (D.E.G.); and by a core facility grant from the National Cancer Institute (CA 14599). This work is dedicated to the memory of Nina Gottschling.

9 August 1994; accepted 27 September 1994